

## Boron Coordination

International Edition: DOI: 10.1002/anie.201509826  
German Edition: DOI: 10.1002/ange.201509826The  $[B_3(NN)_3]^+$  and  $[B_3(CO)_3]^+$  Complexes Featuring the Smallest  $\pi$ -Aromatic Species  $B_3^+$ 

Jiaye Jin, Guanjun Wang, Mingfei Zhou,\* Diego M. Andrada, Markus Hermann, and Gernot Frenking\*

Dedicated to Professor Herbert W. Roesky on the occasion of his 80th birthday

**Abstract:** We report the spectroscopic identification of the  $[B_3(NN)_3]^+$  and  $[B_3(CO)_3]^+$  complexes, which feature the smallest  $\pi$ -aromatic system  $B_3^+$ . A quantum chemical bonding analysis shows that the adducts are mainly stabilized by  $L \rightarrow [B_3L_2]^+$   $\sigma$ -donation.

Much progress has been made in recent years in the synthesis of one- and two-center boron species that exhibit unusual chemical bonds. A tricoordinated borylene complex  $CAAC \rightarrow B(H) \leftarrow CAAC$ , where boron atom is a Lewis base that is stabilized by carbene ligands ( $CAAC$  = cyclic alkyl amino carbene), was synthesized by Bertrand and co-workers.<sup>[1]</sup> The related dicarbonyl complex  $OC \rightarrow B(R) \leftarrow CO$  ( $R$  = bulky aryl group) was recently reported by Braunschweig et al.<sup>[2]</sup> The same group isolated diatomic  $B_2$  in the  $NHC \rightarrow B \equiv B \leftarrow NHC$  ( $NHC$  = N-heterocyclic carbene) complex, which features a boron–boron triple bond.<sup>[3,4a]</sup> They also synthesized the related adducts  $NHC^s \rightarrow B \equiv B \leftarrow NHC^s$  ( $NHC^s$  = saturated  $NHC$ )<sup>[4b]</sup> and  $CAAC \rightarrow B \equiv B \leftarrow CAAC$ .<sup>[4c]</sup> The variation of the  $\pi$ -acceptor strength of the carbene ligands  $L$  modulates the  $L \leftarrow B \equiv B \rightarrow L$   $\pi$ -backdonation, and correlates nicely with the  $B-B$  bond lengths in the complexes<sup>[4]</sup> which supports the model of dative bonding.<sup>[5]</sup> Prior to this, the dicarbonyl complexes  $OC \rightarrow B \equiv B \leftarrow CO$  and  $[OB \rightarrow B \equiv B \leftarrow BO]^{2-}$ , which are molecules with all-triple bonds,<sup>[6]</sup> have been experimentally observed.<sup>[7]</sup>

We now report the extension of stabilizing one- and two-center boron species  $L \rightarrow B_n \leftarrow L$  with donor-ligands  $L$  to three-center cyclic boron complexes  $[B_3(NN)_3]^+$  and  $[B_3(CO)_3]^+$  where the cyclic  $B_3^+$  cation is ligated by three  $N_2$  and  $CO$  ligands, respectively. The eight valence-electron species  $B_3^+$  has two  $\pi$ -electrons which are delocalized over the three-

membered ring and thus, it is the smallest  $\pi$ -aromatic system that has been spectroscopically characterized. The related NHC complex  $[B_3(NHC)_3]^+$  was the subject of a previous theoretical study,<sup>[8]</sup> but it was not observed until now. The molecules  $[B_3(NN)_3]^+$  and  $[B_3(CO)_3]^+$  are the first three-center complexes of main-group atoms that are stabilized through dative bonds by  $CO$  and  $N_2$ . Heavier group-13 homologues of gallium have been synthesized as salt compounds  $[Ga_3R_3][M_2]$  ( $M = Na, K$ ;  $R$  = bulky aryl group), which were the first cyclogallanes that were structurally characterized.<sup>[9]</sup> The related aluminum systems  $[Al_3R_3][M_2]$  have also been isolated.<sup>[10]</sup> Theoretical studies of the parent systems  $[E_3H_3]^{2-}$  ( $E = B, Al, Ga$ ) showed that the dianions are  $2\pi$ -aromatic species,<sup>[9b,11]</sup> similar to the cation  $[B_3L_3]^+$ . The  $[E_3R_3][M_2]$  ( $E = Al, Ga$ ) systems have  $E-R$  electron-sharing bonds, while  $[B_3L_3]^+$  has donor–acceptor bonds. Figure 1 displays the bonding situation in  $[E_3R_3]^{2-}$  and  $[B_3L_3]^+$ .

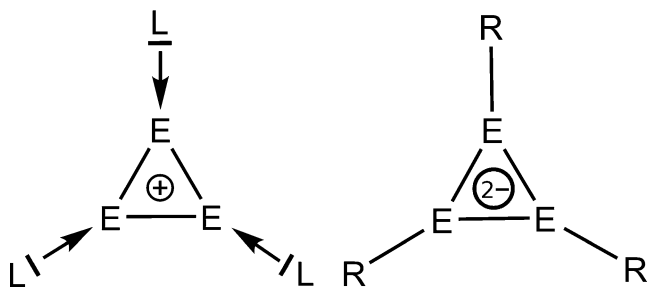


**Figure 1.** Representation of the bonding situation in a) cyclic group-13 cation complex  $[E_3L_3]^+$  which has  $L \rightarrow E$  dative bonds, and b) cyclic group-13 dianion which has  $R-E$  electron-sharing bonds. Both systems are  $2\pi$ -aromatic species.

The boron–dinitrogen and boron–carbonyl cation complexes were generated in the gas phase using a pulsed laser vaporization/supersonic expansion ion source, and were studied by infrared photodissociation spectroscopy in the ligand-stretching vibrational frequency region as described previously.<sup>[12]</sup> A typical mass spectrum of boron dinitrogen cation complexes produced using a  $^{11}B$  target in the  $m/z$  range of 60–160 is shown in Figure 2a. The spectrum is dominated by mononuclear  $BN_n^+$  ( $n = 5–10$ ) cation complexes. Peaks owing to  $[B_2(NN)_3]^+$  and  $[B_3(NN)_3]^+$  are the most intense multinuclear species in the mass spectra. The  $[B_3(NN)_3]^+$

[\*] J. Jin, Prof. G. Wang, Prof. M. Zhou  
Collaborative Innovation Center of Chemistry for Energy Materials  
Department of Chemistry  
Shanghai Key Laboratory of Molecular Catalysts and  
Innovative Materials  
Fudan University  
Shanghai 200433 (China)  
E-mail: mzfzhou@fudan.edu.cn

Dr. D. M. Andrada, Dr. M. Hermann, Prof. G. Frenking  
Fachbereich Chemie, Philipps-Universität Marburg  
Hans-Meerwein-Strasse, 35043 Marburg (Germany)  
E-mail: frenking@chemie.uni-marburg.de

Supporting information for this article is available on the WWW  
under <http://dx.doi.org/10.1002/anie.201509826>.

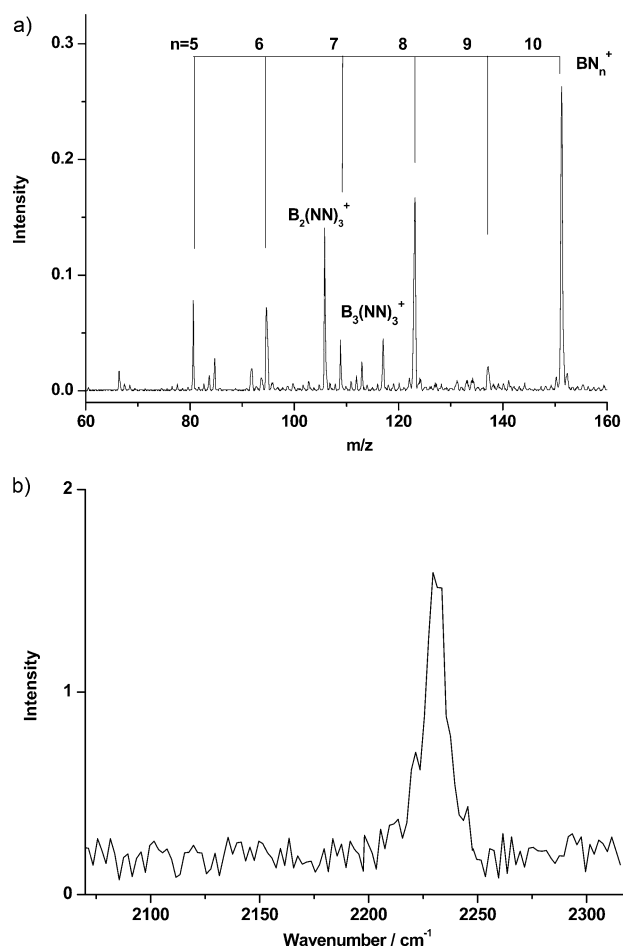


**Figure 2.** a) Mass spectrum of the boron–nitrogen cation complexes. The cations are formed by pulsed laser vaporization of a boron-11 target in an expansion of helium doped with dinitrogen. b) Experimental IR spectrum of the  $[B_3(NN)_3]^+$  cation complex. The spectrum is measured by monitoring the  $N_2$  fragmentation channel leading to the formation of  $[B_3(NN)_2]^+$ .

cation is mass-selected for infrared photodissociation. When the infrared laser is on resonance with one of the vibrational fundamentals of the cation complex, it photodissociates by losing one  $N_2$  ligand with low efficiency (less than 2%). The signal detected is likely due to a multiphoton process, which is not expected to be very efficient at the low laser pulse energies used here (about 2 mJ/pulse). The resulting infrared photodissociation spectrum of  $[B_3(NN)_3]^+$  is shown in Figure 2b. The experimental spectrum exhibits a single band centered at  $2232\text{ cm}^{-1}$ , indicating a high symmetric structure. The band position is shifted by  $98\text{ cm}^{-1}$  to the red from the frequency of gas phase  $N_2$  ( $2330\text{ cm}^{-1}$ ).<sup>[13]</sup>

The mass spectrum of boron–carbonyl cation complexes in the  $m/z$  range of 60–160 is shown in Figure S1. The most intense peaks correspond to  $[B(CO)_3]^+$  and  $[B_2(CO)_4]^+$ , suggesting that these cations are formed preferentially. The  $[B_3(CO)_3]^+$  cation complex is also formed with appreciable intensity. It dissociates by losing a CO ligand when excited with infrared light around the  $2190\text{ cm}^{-1}$  frequency region, but the dissociation efficiency (less than 0.5%; Supporting Information, Figure S2) is too low to achieve an effective

spectrum, indicating that this cation has a higher binding energy than that of  $[B_3(NN)_3]^+$ . Nevertheless, the recorded signal of  $2190\text{ cm}^{-1}$  for the C–O stretching mode suggests a blue shift of  $47\text{ cm}^{-1}$  relative to free CO ( $2143\text{ cm}^{-1}$ ).<sup>[13]</sup>

We carried out high-level ab initio calculations of  $[B_3(NN)_3]^+$  and  $[B_3(CO)_3]^+$  using coupled-cluster theory at the CCSD(T)/cc-pVTZ level<sup>[14]</sup> to validate the identity of the cations and to analyze their electronic structure. Figure 3a shows the theoretically predicted geometries of the two complexes and the fragments ( $X^1A_1'$ )  $B_3^+$ ,  $N_2$ , and CO. The calculated bond lengths of the diatomic species agree very well with experimental data. Previous theoretical studies showed that  $B_3^+$  has a  $D_{3h}$  equilibrium geometry and an  $X^1A_1'$  electronic ground state.<sup>[15]</sup> Alexandrova and co-workers

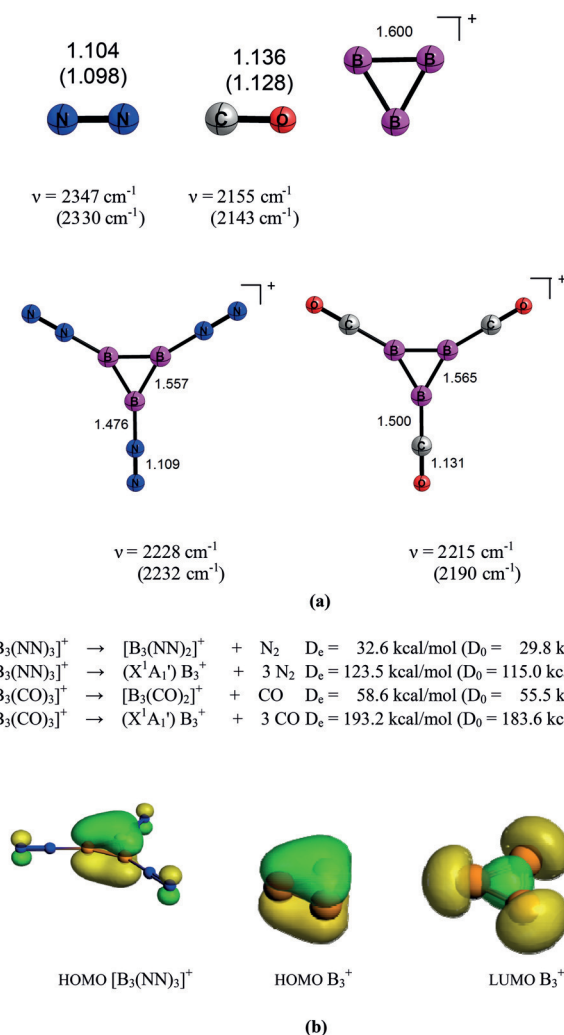


**Figure 3.** a) Calculated (experimental) equilibrium geometries of the complexes  $[B_3(NN)_3]^+$  and  $[B_3(CO)_3]^+$  and the fragments ( $X^1A_1'$ )  $B_3^+$ ,  $N_2$ , and CO at CCSD(T)/cc-pVTZ. Bond lengths are given in Å. Calculated (experimental) vibrational frequencies of the N–N and C–O stretching modes at LCCSD(T)/cc-pVTZ. Experimental values for  $N_2$  and CO were taken from Ref. [13]. Calculated bond dissociation energies  $D_e$  and  $D_0$  at CCSD(T)/cc-pVTZ. The zero-point energy corrections were taken from LCCSD(T)/cc-pVTZ calculations. b) Plot of molecular orbitals at BP86/TZ2P+: HOMO of  $[B_3(NN)_3]^+$ , HOMO of ( $X^1A_1'$ )  $B_3^+$  and LUMO of ( $X^1A_1'$ )  $B_3^+$ .

mention in a review about neutral and charged all-boron clusters  $B_n^q$  ( $n=2-6$ ) that  $B_3^+$  is a  $2\pi$ -aromatic species.<sup>[16]</sup>

The calculations suggest that the B–B lengths in the complexes  $[B_3L_3]^+$  are significantly shorter (1.557 Å for  $L=N_2$  and 1.565 Å for  $L=CO$ ) than in free  $B_3^+$  (1.600 Å). Also, the N–N bonds in  $[B_3(NN)_3]^+$  (1.109 Å) are a bit longer than in  $N_2$  (1.104 Å), while the C–O bond in  $[B_3(CO)_3]^+$  becomes a bit shorter (1.131 Å) compared with CO (1.136 Å). We calculated the vibrational spectra of the complexes using local coupled-cluster theory at the LCCSD(T)/cc-pVTZ level,<sup>[14]</sup> because frequency calculations at CCSD(T)/cc-pVTZ are not feasible for us. The optimized geometries of the molecules at LCCSD(T)/cc-pVTZ are very similar to the CCSD(T)/cc-pVTZ structures (Supporting Information). The computed stretching modes at LCCSD(T)/cc-pVTZ are in agreement with the changes of the bond lengths in  $[B_3L_3]^+$ : a red shift of the highest-lying IR active N–N stretching mode<sup>[17]</sup> of  $\Delta\nu = 119\text{ cm}^{-1}$  for  $[B_3(NN)_3]^+$ , while the C–O stretching frequency of  $[B_3(CO)_3]^+$  exhibits a blue-shift by  $\Delta\nu = 60\text{ cm}^{-1}$  (Figure 3). The excellent agreement of the size and the direction of the C–O and N–N frequency shifts  $\Delta\nu$  strongly supports the assignment of the complexes  $[B_3(NN)_3]^+$  and  $B_3(CO)_3^+$  to the spectroscopic data. The complete data of the calculated vibrational frequencies are given in the Supporting Information (Table S1). Figure 3 also shows the calculated bond dissociation energies (BDEs) for loss of one or three ligands  $L$  from  $[B_3L_3]^+$ . The calculations suggest that the CO ligands are more strongly bonded than  $N_2$ , which agrees with the smaller efficiency of the photodissociation.

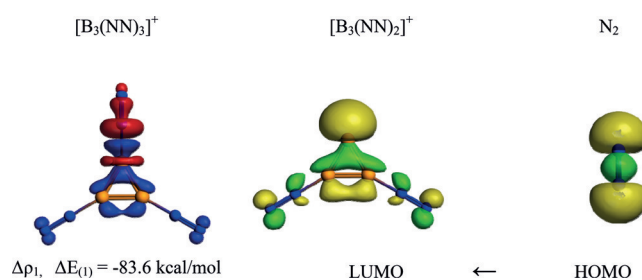
Figure 3b shows a plot of the highest occupied molecular orbital (HOMO) of  $[B_3(NN)_3]^+$  which resembles the undisturbed HOMO of naked ( $X^1A_1'$ )  $B_3^+$  that is also shown. The equivalent HOMO of  $[B_3(CO)_3]^+$  looks very similar (Supporting Information, Figure S3). The shape of the HOMO indicates that the all-boron systems  $B_3^+$  and  $[B_3L_3]^+$  are two  $\pi$ -electron aromatic species. We estimated the aromaticity in the molecules with the nuclear independent chemical shift (NICS) method<sup>[18]</sup> and compared it with the classical two  $\pi$ -electron aromatic cyclopropenyl cation  $C_3H_3^+$ . The calculated NICS(1) values, which were suggested as reliable indicators of aromaticity in non-fused cyclic systems,<sup>[19]</sup> predict that all-boron cations possess significant aromatic character with decreasing order  $B_3^+$  (–18.4 ppm) >  $C_3H_3^+$  (–14.6 ppm) >  $[B_3(CO)_3]^+$  (–13.2 ppm) >  $[B_3(NN)_3]^+$  (–11.6 ppm).<sup>[20]</sup>

Figure 3b shows the lowest unoccupied molecular orbital (LUMO) of naked ( $X^1A_1'$ )  $B_3^+$ , which is perfectly suited for  $L_3 \rightarrow B_3^+$   $\sigma$ -donation. We analyzed the nature of the donor–acceptor bonds of  $[B_3(NN)_3]^+$  and  $[B_3(CO)_3]^+$  with the energy decomposition analysis with natural orbitals of chemical valence (EDA-NOCV)<sup>[21]</sup> method.<sup>[22]</sup> The numerical results are given in Table 1. The strongest attraction between the ligand and the remaining fragment  $L \rightarrow [B_3L_2]^+$  comes from the orbital interactions  $\Delta E_{\text{orb}}$ . The largest contribution to  $\Delta E_{\text{orb}}$  arises from the  $\sigma$ -donation of the lone-pair orbitals of the ligands  $N_2$  and CO to the LUMO of ( $X^1A_1'$ )  $B_3^+$ . This is nicely shown in Figure 4 which depicts the deformation

**Table 1:** Energy decomposition analysis of  $[B_3L_3]^+$  at the BP86/TZ2P+ level using CCSD(T)/cc-pVTZ optimized geometries. Energy values are given in kcal mol<sup>–1</sup>.

Fragments	$[B_3(NN)_2]^+ + N_2$	$[B_3(CO)_2]^+ + CO$
$\Delta E_{\text{int}}$	–50.7	–76.9
$\Delta E_{\text{Pauli}}$	171.6	202.4
$\Delta E_{\text{elstat}}^{\text{[a]}}$	–79.3 (35.6%)	–100.2 (35.9%)
$\Delta E_{\text{orb}}^{\text{[a]}}$	–143.0 (64.3%)	–179.1 (64.1%)
$\Delta E_{\text{orb}}(1)^{\text{[b]}}$ $L \rightarrow [B_3(L)_2]^+$ $\sigma$ -donation	–83.6 (58.5%)	–112.3 (62.7%)
$\Delta E_{\text{orb}}(2)^{\text{[b]}}$ $L \leftarrow [B_3(L)_2]^+$ $\pi_{\parallel}$ -backdonation	–20.3 (14.2%)	–26.7 (14.9%)
$\Delta E_{\text{orb}}(3)^{\text{[b]}}$ $L \leftarrow [B_3(L)_2]^+$ $\pi_{\perp}$ -backdonation	–18.5 (12.9%)	–19.6 (10.9%)
$\Delta E_{\text{orb}}(\text{rest})^{\text{[b]}}$ polarization	–20.6 (14.4%)	–20.5 (12.2%)

[a] The value in parentheses gives the percentage contribution to the total attractive interactions  $\Delta E_{\text{elstat}} + \Delta E_{\text{orb}}$ . [b] The value in parentheses gives the percentage contribution to the total orbital interactions  $\Delta E_{\text{orb}}$ .



**Figure 4.** Plot of the deformation densities  $\Delta\rho$  of the pairwise orbital interactions between  $[B_3(NN)_2]^+$  and  $N_2$  in  $[B_3(NN)_3]^+$  and associated stabilization energies  $\Delta E$  in kcal mol<sup>–1</sup>. The color code of the charge flow is red  $\rightarrow$  blue. Shape of the most important interacting orbitals of  $[B_3(NN)_2]^+$  and  $N_2$ .

density  $\Delta\rho$  that is associated with the  $\sigma$ -donation  $NN \rightarrow [B_3(NN)_2]^+$  in the dinitrogen complex. The color code for the charge flow is red  $\rightarrow$  blue. The connected donor and acceptor orbitals of the fragments  $N_2$  and  $[B_3(NN)_2]^+$  are also shown in Figure 4. The shape of the deformation densities and the associated orbitals reveal that the  $NN \rightarrow [B_3(NN)_2]^+$   $\sigma$ -donation enhances also the B–B bonding in the ring which explains the bond shortening with respect to free ( $X^1A_1'$ )  $B_3^+$ . Note that the  $L \leftarrow [B_3L_2]^+$   $\pi$ -backdonation (Table 1) which comes from the in-plane  $\pi_{\parallel}$  orbital is stronger (–20.3 kcal mol<sup>–1</sup> for  $L=N_2$  and –26.7 kcal mol<sup>–1</sup> for  $L=CO$ ) than the contribution of the out-of-plane  $\pi_{\perp}$  MO (–18.5 kcal mol<sup>–1</sup> for  $L=N_2$  and –19.6 kcal mol<sup>–1</sup> for  $L=CO$ ) which is the source of the aromaticity. The deformation densities  $\Delta\rho$  and the associated fragments orbitals for the  $L \leftarrow [B_3(NN)_2]^+$   $\pi$ -backdonation and the donation and backdonation in  $[B_3(CO)_3]^+$  are shown in the Supporting Information (Figure S4).

The elongation of the N–N bonds in the complex  $[B_3(NN)_3]^+$  relative to free  $N_2$  can be explained with the N–N bonding nature of the  $\sigma$ -donor orbital and the antibonding  $\pi^*$ -acceptor orbital of dinitrogen. The bond-shortening of the C–O bond in non-classical carbonyl complexes,<sup>[23]</sup> where CO is mainly a  $\sigma$ -donor, has been shown to come from the change in the polarization of the orbitals when electronic charge is withdrawn from the carbon atom.<sup>[24]</sup> A similar effect has recently been observed in the complex  $[OC(BeCO_3)]$ , where the origin of the C–O bond shortening was discussed in detail.<sup>[22]</sup> The atomic partial charges of the NBO method<sup>[25]</sup>



agree with the strong  $\sigma$ -donation in the complexes. The partial charge at the cyclic  $B_3$  moiety is  $-0.06$  e in  $[B_3(NN)_3]^+$ , which indicates that the positive charge of the cation is completely localized at the more electronegative dinitrogen ligands. Even stronger donation  $3CO \rightarrow B_3^+$  is found in the tricarbonyl complex  $[B_3(CO)_3]^+$ , where the partial charge of  $B_3$  is  $-0.38$  e.

It is illuminating to compare the bonding situation in  $B_3^+$  and  $[B_3L_3]^+$  with  $B_3^-$ . The latter anion has two more electrons than the cation, and thus the LUMO of  $B_3^+$  (Figure 3b) is occupied in  $B_3^-$  where it becomes the HOMO. The latter orbital has been declared as the source of  $\sigma$  aromaticity, because it is a delocalized  $2\sigma$  electron system that apparently agrees with the  $4n+2$  rule.<sup>[16,26]</sup> Therefore, it is claimed that  $B_3^-$  is a double ( $\sigma$  and  $\pi$ ) aromatic species, while  $B_3^+$  exhibits  $2\pi$  aromaticity but no  $\sigma$  aromaticity.<sup>[16,27]</sup> It may now be argued that  $[B_3L_3]^+$  also possesses some  $\sigma$  aromaticity, because the  $L \rightarrow B$  interaction leads to partial occupation of the LUMO of  $B_3^+$ . We refrain from discussing the possible degree of  $\sigma$  aromaticity in  $[B_3L_3]^+$  because we are not convinced that the stabilization has a genuine aromatic origin. There is no doubt that there is some stabilization in the  $B_3^+$  fragment of the complex that comes from the partial occupation of the delocalized LUMO of the cation. This can be seen from the shortening of the B–B bonds. However, delocalization does not automatically indicate aromaticity. The  $B_3^-$  has a total of four doubly occupied  $\sigma$  orbitals, which makes it an  $8\sigma$  electron system that would be an antiaromate according to the Hückel rule. It is somewhat artificial to discard the three lower-lying  $\sigma$  orbitals and to declare it a  $2\sigma$  aromate. But there is no doubt that  $[B_3(NN)_3]^+$  and  $[B_3(CO)_3]^+$  are genuine  $2\pi$  aromatic species.

After this manuscript was submitted, a work by Braunschweig and co-workers appeared that reported the synthesis of the triboracyclopropenyl dianion  $[B_3(NCy)_3]^{2-}$  (Cy = cyclo- $C_6H_{11}$ ) which was isolated as the dimeric salt  $(Na_4[B_3(NCy)_3]_2 \cdot 2DME)$  where  $DME = 1,2$ -dimethoxyethane.<sup>[28]</sup> The molecule is the boron analogue of the heavier systems  $[E_3R_3][M_2]$  ( $E = Al, Ga$ ).<sup>[9,10]</sup> The bonding analysis gave clear evidence that  $[B_3(NCy)_3]^{2-}$  is a Hückel  $2\pi$  aromate. The latter dianion and the  $[B_3L_3]^+$  cations that are reported here exhibit the bonding situations that are shown in Figure 1. They are examples of the lightest possible main-group element Hückel  $\pi$  aromate.<sup>[29]</sup> It is interesting that the  $2\pi$  aromaticity is found in both the eight-electron cation  $B_3^+$  and in the eleven-electron dianion  $B_3^{2-}$ .

In summary, we report the first spectroscopic identification of the complexes  $[B_3(NN)_3]^+$  and  $[B_3(CO)_3]^+$ , which feature the smallest  $\pi$ -aromatic system  $B_3^+$ . A quantum chemical bonding analysis shows that the adducts are mainly stabilized by  $L \rightarrow [B_3L_2]^+$   $\sigma$ -donation. The results may be considered as exploration of a new field of ligand-stabilized boron complexes  $B_3L_3$ , which may be extended to main-group adducts  $E_nL_n$  with other atoms and ligands and larger cycles.

## Acknowledgements

The work at Shanghai was supported by the Ministry of Science and Technology of China (2013CB834603 and

2012YQ220113-3) and the National Natural Science Foundation of China (grant no. 21433005). The work at Marburg was supported by the Deutsche Forschungsgemeinschaft.

**Keywords:** aromaticity · bonding analysis · coordination chemistry · photodissociation · physical chemistry

**How to cite:** *Angew. Chem. Int. Ed.* **2016**, 55, 2078–2082  
*Angew. Chem.* **2016**, 128, 2118–2122

- [1] R. Kinjo, B. Donnadieu, M. A. Celik, G. Frenking, G. Bertrand, *Science* **2011**, 333, 610.
- [2] a) H. Braunschweig, R. D. Dewhurst, F. Hupp, M. Nutz, K. Radacki, C. W. Tate, A. Vargas, Y. Ye, *Nature* **2015**, 522, 327; b) G. Frenking, *Nature* **2015**, 522, 297.
- [3] The assignment of a BB triple bond was challenged by: a) R. Köppe, H. Schnöckel, *Chem. Sci.* **2015**, 6, 1199; The arguments in that paper were shown to be faulty by: b) N. Holzmann, M. Hermann, G. Frenking, *Chem. Sci.* **2015**, 6, 4089; See also: c) J. Böhnke, H. Braunschweig, P. Constantinidis, T. Dellermann, W. C. Ewing, I. Fischer, K. Hammond, F. Hupp, J. Mies, H.-C. Schmitt, A. Vargas, *J. Am. Chem. Soc.* **2015**, 137, 1766; d) F. A. Perras, W. C. Ewing, T. Dellermann, J. Böhnke, S. Ulrich, T. Schäfer, H. Braunschweig, D. L. Bryce, *Chem. Sci.* **2015**, 6, 3378.
- [4] a) H. Braunschweig, R. D. Dewhurst, K. Hammond, J. Mies, K. Radacki, A. Vargas, *Science* **2012**, 336, 1420; b) J. Böhnke, H. Braunschweig, W. C. Ewing, C. Hörl, T. Kramer, I. Krumm-nacher, J. Mies, A. Vargas, *Angew. Chem. Int. Ed.* **2014**, 53, 9082; *Angew. Chem.* **2014**, 126, 9228; c) J. Böhnke, H. Braunschweig, T. Dellermann, W. C. Ewing, K. Hammond, T. Kramer, J. O. C. Jimenez-Halla, J. Mies, *Angew. Chem. Int. Ed.* **2015**, 54, 13801–13805; *Angew. Chem.* **2015**, 127, 14006–14010.
- [5] G. Frenking, *Angew. Chem. Int. Ed.* **2014**, 53, 6040; *Angew. Chem.* **2014**, 126, 6152.
- [6] L. C. Ducati, N. Takagi, G. Frenking, *J. Phys. Chem. A* **2009**, 113, 11693.
- [7] a) M. Zhou, N. Tsumori, Z. Li, K. Fan, L. Andrews, Q. Xu, *J. Am. Chem. Soc.* **2001**, 123, 12936; b) S. Li, H. Zhai, L. Wang, *J. Am. Chem. Soc.* **2008**, 130, 2573.
- [8] T. B. Tai, M. T. Nguyen, *Angew. Chem. Int. Ed.* **2013**, 52, 4554; *Angew. Chem.* **2013**, 125, 4652.
- [9] a) X.-W. Li, W. T. Pennington, G. H. Robinson, *J. Am. Chem. Soc.* **1995**, 117, 7578; b) X.-W. Li, Y. Xie, P. Schreiner, K. D. Gripper, R. C. Crittendon, C. Campana, H. F. Schaefer III, G. H. Robinson, *Organometallics* **1996**, 15, 3798.
- [10] R. J. Wright, M. Brynda, P. P. Power, *Angew. Chem. Int. Ed.* **2006**, 45, 5953; *Angew. Chem.* **2006**, 118, 6099.
- [11] X. Li, J. Sun, Y. Zeng, Z. Sun, S. Zheng, L. Meng, *J. Phys. Chem. A* **2012**, 116, 5491.
- [12] G. J. Wang, C. X. Chi, X. P. Xing, C. F. Ding, M. F. Zhou, *Sci. China Chem.* **2014**, 57, 172.
- [13] K. P. Huber, G. Herzberg, *Constants of Diatomic Molecules*, Van Nostrand-Reinhold, New York, **1979**.
- [14] See the Supporting Information for the details of the calculations.
- [15] C. L. Yang, Z. H. Zhu, *J. Mol. Struct.* **2001**, 571, 225.
- [16] A. N. Alexandrova, A. I. Boldyrev, H.-J. Zhai, L.-S. Wang, *Coord. Chem. Rev.* **2006**, 250, 2811.
- [17] There is one degenerate N–N and C–O stretching mode in the complexes that is IR active, and one non-degenerate stretching mode that is IR inactive. See the Supporting Information for the full spectra.
- [18] P. v. R. Schleyer, C. Maerker, A. Dransfeld, H. Jiao, N. J. R. von Hommes, *J. Am. Chem. Soc.* **1996**, 118, 6317.
- [19] P. v. R. Schleyer, H. Jiao, N. J. R. von Hommes, V. G. Malkin, O. L. Malkina, *J. Am. Chem. Soc.* **1997**, 119, 12669.

- [20] A theoretical study by Tsipis et al. suggested that cyclic  $B_3^+$  is actually a  $\sigma$ -aromatic compound. The conclusion was made on the basis of the NICS<sub>zz</sub> scan of the molecule, which is symmetric around the z-axis that is perpendicular to the molecular plane: A. C. Tsipis, I. G. Depastas, C. A. Tsipis, *Symmetry* **2010**, 2, 284. We rather consider  $B_3^+$  to be a  $2\pi$  aromate, because the molecule has a delocalized  $\pi$  orbital which is occupied by two electrons.
- [21] A. Michalak, M. Mitoraj, T. Ziegler, *J. Phys. Chem. A* **2008**, 112, 1933.
- [22] For a recent application of the EDA-NOCV method to a related carbonyl complex see: M. Chen, Q. Zhang, M. Zhou, D. M. Andrada, G. Frenking, *Angew. Chem. Int. Ed.* **2015**, 54, 124; *Angew. Chem.* **2015**, 127, 126.
- [23] A. J. Lupinetti, G. Frenking, S. H. Strauss, *Angew. Chem. Int. Ed.* **1998**, 37, 2113; *Angew. Chem.* **1998**, 110, 2229.
- [24] A. J. Lupinetti, G. Frenking, S. H. Strauss, *J. Phys. Chem. A* **1997**, 101, 9551.
- [25] C. R. Landis, F. Weinhold, *Valency and Bonding: A Natural Bond Orbital Donor-Acceptor Perspective*, Cambridge University Press, Cambridge, **2005**.
- [26] A. E. Kuznetsov, A. I. Boldyrev, *Struct. Chem.* **2002**, 13, 141.
- [27] A. I. Boldyrev, L. S. Wang, *Chem. Rev.* **2005**, 105, 3716.
- [28] T. Kupfer, H. Braunschweig, K. Radacki, *Angew. Chem. Int. Ed.* **2015**, 54, 15084; *Angew. Chem.* **2015**, 127, 15299.
- [29] One referee objected to the classification of  $[B_3L_3]^+$  as “the lightest possible main-group element Hückel  $\pi$  aromate” that was synthesized, because the inclusion of the ligand atoms L makes the compounds  $[B_3(NN)_3]^+$  and  $[B_3(CO)_3]^+$  bigger than the deltate anion  $[C_3O_3]^{2-}$  reported earlier by West et al. We disagree, because the aromaticity in  $[B_3L_3]^+$  is due to the electronic structure of the core moiety  $B_3^+$  where the ligands L serve merely to stabilize the aromatic cation. In contrast, the aromaticity in  $[C_3O_3]^{2-}$  requires the presence of the oxygen atoms whose  $\pi$ -interactions are necessary to make the ion being a  $\pi$  aromate: R. West, D. Eggerding, J. Perkins, D. Handy, E. C. Tuazon, *J. Am. Chem. Soc.* **1979**, 101, 1710; J.-I. Aihara, *J. Am. Chem. Soc.* **1981**, 103, 1633; X. Bao, X. Zhou, C. F. Lovitt, A. Venkatram, D. A. Hrovat, R. Gleiter, R. Hoffmann, W. T. Borden, *J. Am. Chem. Soc.* **2013**, 135, 10259, and references therein.

Received: October 20, 2015

Revised: December 7, 2015

Published online: January 6, 2016